Generation of a novel spherical chaotic attractor from a new three-dimensional system*

Sun Chang-Chun(孙常春)†, Zhao En-Liang(赵恩良), and Xu Qi-Cheng(徐启程)

School of Science, Shenyang Jianzhu University, Shenyang 110168, *China*

(Received 6 September 2013; revised manuscript received 5 November 2013; published online 25 March 2014)

A new three-dimensional (3D) system is constructed and a novel spherical chaotic attractor is generated from the system. Basic dynamical behaviors of the chaotic system are investigated respectively. Novel spherical chaotic attractors can be generated from the system within a wide range of parameter values. The shapes of spherical chaotic attractors can be impacted by the variation of parameters. Finally, a simpler 3D system and a more complex 3D system with the same capability of generating spherical chaotic attractors are put forward respectively.

Keywords: three-dimensional system, spherical chaotic attractor, chaos generation

PACS: 05.45.Gg, 05.45.–a, 05.45.Pq **DOI:** 10.1088/1674-1056/23/5/050505

1. Introduction

It is well known that chaos can be found in some three-dimensional (3D) or higher-dimensional continuous nonlinear dynamical systems. In 1963, Lorenz[1] found the first chaotic system in 3D continuous autonomous nonlinear systems. Subsequently, with the development of computer science and technology, several classes of representative continuous chaotic systems including the Rössler[2] system, Chua[3] system, Sprott[4] system, Chen[5] system, and Lü[6] system were found successively. So far, many new continuous chaotic or hyperchaotic systems have been found and basic dynamical behaviors of the systems have been investigated by researchers.[7–36]

The shapes of chaotic attractors are various. Two classes of representative shapes are wing-shaped and scroll-shaped. The attractors of the Lorenz[1] system, Chen[5] system, and Lü[6] system are double-wing attractors. A novel and single four-wing chaotic attractor can be generated from a new 3D quadratic autonomous system with five system parameters and three quadratic cross-product terms.[7] A four-wing hyperchaotic attractor and a pair of coexistent double-wing hyperchaotic attractors with two symmetrical initial conditions can be generated from a new four-dimensional (4D) smooth quadratic autonomous chaotic system.[8] A novel four-wing-hyper-chaotic attractor can be generated from a new hyper-chaotic system with one equilibrium point as the parameter varies.[9] By employing a nonlinear state feedback controller, a new simple 4D chaotic system is proposed and a four-wing chaotic attractor in all directions can be generated.[10] A new 3D four-wing chaotic system with cubic nonlinearity is put forward and physically implemented.[11] Dadras *et al.*[12] presented a new 3D quadratic autonomous chaotic system that can generate one-wing, two-wing, three-wing, and four-wing chaotic attractors and two coexisting one-wing and two coexisting two-wing attractors with different initial conditions. In 2011, Yu *et al.*[13] proposed a novel 4D autonomous chaotic system that can generate one-wing, two-wing, three-wing, and four-wing chaotic attractors with the variation of a single parameter.

Multi-wing chaotic attractors can be generated by constructing a piecewise function. The N-wing and $n\times m$-wing Lorenz-like attractors can be generated from a modified Shimizu–Morioka model.[14] Grid multi-wing chaotic attractors can be generated from the multi-piecewise Lü system by constructing a heteroclinic loop and a switching control.[15] A new grid multi-wing chaotic system is constructed by modifying a double-wing chaotic system and an oscillator circuit is designed for implementation.[16] By employing the statistical complexity measure (SCM) and the spectral entropy (SE) algorithm, the complexities of multi-wing chaotic systems based on the modified Chen system and a multi-segment quadratic function are investigated.[17] Based on a 3D Lorenz system, a 4D multi-wing chaotic system by appending a state variable and a piecewise linear function is constructed and multi-wing butterfly chaotic attractors are generated.[18]

Most of the scroll-shaped attractors were generated by constructing a piecewise function and employing a switching approach. The attractor of the Chua[3] system is a double-scroll attractor. In 2000, Sprott[19] designed a new class of chaotic circuits with the capability of generating a double-scroll attractor. A three-scroll attractor was generated from a 3D quadratic autonomous chaotic system.[20] N-scroll chaotic attractors can be generated from a linear system by designing a switching scalar output feedback controller.[21] Multi-

*Project supported by the Science Research Foundation of Liaoning Provincial Education Department, China (Grant No. L2013229).

†Corresponding author. E-mail: changchunsun@sina.com

© 2014 Chinese Physical Society and IOP Publishing Ltd

scroll chaotic attractors can be generated from a 3D continuous system and be implemented by a circuit.[22] Lü *et al.*[23–26] presented three novel switching approaches to generate multi-scroll chaotic attractors. The approaches included a saturated function series, hysteresis function series, and thresholding. Yu *et al.* put forward a novel nonlinear modulating function approach for generating N-scroll chaotic attractors based on a general jerk circuit in Ref. [27] and presented a discrete and extended transformation approach for generating N-scroll hyperchaotic attractors based on a generalized Matsumoto–Chua–Kobayashi (MCK) circuit in Ref. [28]. In 2010, Zhang and Yu developed a novel switching piecewise-linear (PWL) controller approach for generating grid multi-scroll chaotic attractors.[29]

The other shapes of known chaotic attractors included basin-shaped,[30–32] torus-shaped,[33] funnel-shaped,[34] rectangular,[35] and so on.

In 2004, Zhou and Chen found firstly a three-layer attractor generated from a new simple smooth quadratic autonomous chaotic system with four unstable equilibrium points and three homoclinic orbits.[36] The new found system with nine parameters and three quadratic cross-product terms had a strong capability of generating an embedded umbrella-ball attractor and an embedded multi-ball attractor.

In this paper, a new 3D continuous autonomous chaotic system with eight parameters and two quadratic terms is constructed. Two quadratic terms are composed of a quadratic cross-product term and a quadratic square term. A novel spherical chaotic attractor can be generated from the chaotic system with three constant terms. Basic dynamical behaviors including symmetry and dissipation, system equilibria, the directions of system orbit and the variation of parameters are investigated respectively. Plenty of novel spherical chaotic attractors can be generated from the system within a wide range of parameter values. The shapes of spherical chaotic attractors can be impacted by the variation of parameters and the corresponding simulations show the process of evolvement. Finally, a simpler 3D system and a more complex 3D system with the same capability of generating spherical chaotic attractors are presented further.

2. A novel spherical chaotic attractor

Consider a new 3D continuous autonomous system with eight parameters and two quadratic terms

$$\begin{cases} \dot{x} = a_1 x + b_1 y + c_1, \\ \dot{y} = a_2 x + b_2 yz + c_2, \\ \dot{z} = a_3 y^2 + c_3, \end{cases} \tag{1}$$

where a_i, b_j, c_k are system parameters, $a_1 < 0$, $a_2 b_1 < 0$, $b_2 > 0$, $a_3 < 0$, $c_3 > 0$, $i = 1,2,3$; $j = 1,2$; $k = 1,2,3$.

When $a_1 = -1$, $b_1 = 80$, $c_1 = 18$, $a_2 = -80$, $b_2 = 1$, $c_2 = -18$, $a_3 = -1$, $c_3 = 60$, the initial value $(x_0, y_0, z_0) = (2,2,2)$, the system (1) has a novel spherical chaotic attractor (see Figs. 1–4).

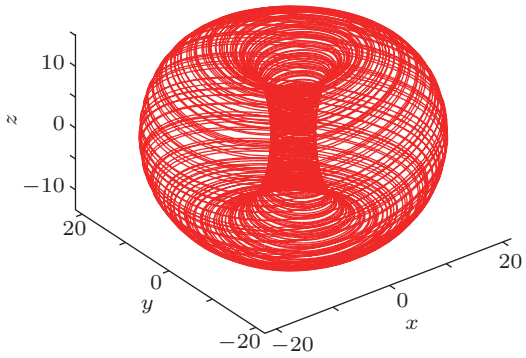


Fig. 1. (color online) A novel spherical chaotic attractor.

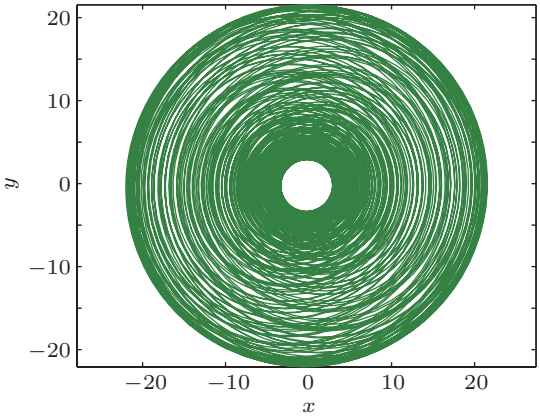


Fig. 2. (color online) Projection of the chaotic attractor in the x–y plane.

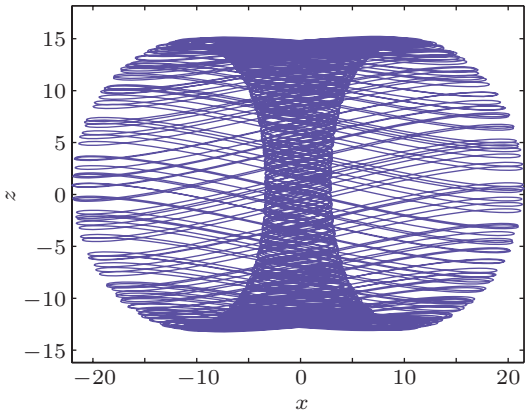


Fig. 3. (color online) Projection of the chaotic attractor in the x–z plane.

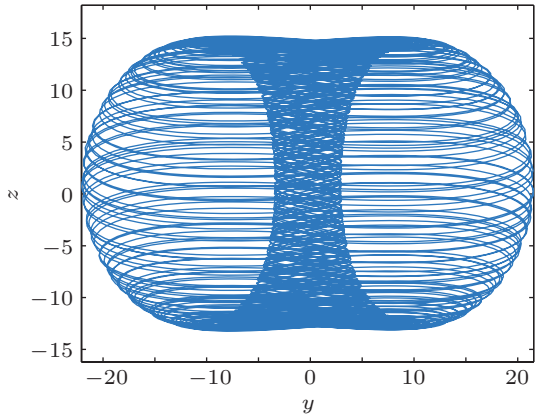


Fig. 4. (color online) Projection of the chaotic attractor in the y–z plane.

3. Analysis of basic dynamical behaviors

Basic dynamical behaviors of the system (1) are investigated in detail by theoretical analysis and numerical simulations.

3.1. Symmetry and dissipation

When $c_1^2 + c_2^2 \neq 0$, the system (1) has a dissymmetry under any coordinate transformation.

When $c_1 = c_2 = 0$, the system (1) has a natural symmetry under the coordinate transformation $(x, y, z) \to (-x, -y, z)$. It means that the system (1) has a rotation symmetry around the z axis.

The divergence of the system (1) is defined by

$$\nabla V = \frac{\partial \dot{x}}{\partial x} + \frac{\partial \dot{y}}{\partial y} + \frac{\partial \dot{z}}{\partial z} = a_1 + b_2 z. \tag{2}$$

When $z < -a_1/b_2$, we have $\nabla V < 0$, the system (1) is dissipative.

3.2. System equilibria

The system (1) has two equilibria by solving the equations $\dot{x} = \dot{y} = \dot{z} = 0$, which are described respectively as follows:

$$\left(-\frac{c_1 + b_1\sqrt{-c_3/a_3}}{a_1}, \sqrt{-\frac{c_3}{a_3}}, \frac{-c_2 + a_2(c_1 + b_1\sqrt{-c_3/a_3})/a_1}{b_2\sqrt{-c_3/a_3}} \right),$$
$$\left(-\frac{c_1 - b_1\sqrt{-c_3/a_3}}{a_1}, -\sqrt{-\frac{c_3}{a_3}}, \frac{c_2 - a_2(c_1 - b_1\sqrt{-c_3/a_3})/a_1}{b_2\sqrt{-c_3/a_3}} \right).$$

The Jacobian matrix $\boldsymbol{J}$ of the system (1) is

$$\boldsymbol{J} = \begin{bmatrix} a_1 & b_1 & 0 \\ a_2 & b_2 z & b_2 y \\ 0 & 2a_3 y & 0 \end{bmatrix} = \begin{bmatrix} \boldsymbol{A} & \boldsymbol{B} \\ \boldsymbol{C} & 0 \end{bmatrix}, \tag{3}$$

where

$$\boldsymbol{A} = \begin{bmatrix} a_1 & b_1 \\ a_2 & b_2 z \end{bmatrix}, \quad \boldsymbol{B} = \begin{bmatrix} 0 \\ b_2 y \end{bmatrix}, \quad \boldsymbol{C} = \begin{bmatrix} 0 & 2a_3 y \end{bmatrix}.$$

It is obvious that the structure of matrix $\boldsymbol{J}$ is independent to the parameters c_j, $j = 1, 2, 3$.

3.3. System orbit

In order to describe the directions of system orbit, matrix $\boldsymbol{A}$ in the Jacobian matrix $\boldsymbol{J}$ is investigated firstly. Assume that matrix $\boldsymbol{A}$ has a pair of conjugate complex eigenvalues $\lambda_{1,2} = a \pm b\mathrm{j}$, where $b > 0$, $\mathrm{j}^2 = -1$. For $\forall z$, the following two equations hold

$$\mathrm{tr}(\boldsymbol{A}) = \lambda_1 + \lambda_2 = a_1 + b_2 z = 2a, \tag{4}$$
$$\det(\boldsymbol{A}) = \lambda_1 \lambda_2 = a_1 b_2 z - a_2 b_1 = a^2 + b^2, \tag{5}$$

where $\mathrm{tr}(\boldsymbol{A})$, $\det(\boldsymbol{A})$ are the trace and determinant of matrix $\boldsymbol{A}$ respectively. By solving Eqs. (4) and (5), we have

$$a = \frac{a_1 + b_2 z}{2}, \quad b = \frac{\sqrt{-4a_2 b_1 - a_1^2 + 2a_1 b_2 z - b_2^2 z^2}}{2}.$$

For $\forall z$, the following inequality holds

$$-4a_2 b_1 - a_1^2 + 2a_1 b_2 z - b_2^2 z^2 > 0. \tag{6}$$

According to the inequality (6), we have

$$|a_1 - b_2 z| < 2\sqrt{-a_2 b_1}. \tag{7}$$

If the following inequality

$$|z| < \frac{2\sqrt{-a_2 b_1} - |a_1|}{|b_2|} \tag{8}$$

holds, then the inequalities (6) and (7) hold.

Since that the system (1) is a chaotic system, therefore, the variable z is norm-bounded. Assume that there exists a positive real constant $M > 0$, such that the following inequalities hold simultaneously:

$$|z| < M \leq \frac{2\sqrt{-a_2 b_1} - |a_1|}{|b_2|}. \tag{9}$$

If inequalities (9) hold, for $\forall z$, then matrix $\boldsymbol{A}$ has a pair of conjugate complex eigenvalues. In order to satisfy this condition, the values of parameters a_1, a_2, b_1, and b_2 can be modulated within a wide range. A potential and simple approach is that $-a_2 b_1$ is large enough and $|a_1|$, $|b_2|$ are small enough.

The following results on the system orbit are obtained easily under the premise that matrix $\boldsymbol{A}$ has a pair of conjugate complex eigenvalues.

1) When $b_1 > 0$ and $a_1 + b_2 z > 0$, the system orbit observed from the positive z half-axis to the x–y plane is clockwise and divergent.

2) When $b_1 > 0$ and $a_1 + b_2 z < 0$, the system orbit observed from the positive z half-axis to the x–y plane is clockwise and convergent.

3) When $b_1 < 0$ and $a_1 + b_2 z > 0$, the system orbit observed from the positive z half-axis to the x–y plane is counterclockwise and divergent.

4) When $b_1 < 0$ and $a_1 + b_2 z < 0$, the system orbit observed from the positive z half-axis to the x–y plane is counterclockwise and convergent.

It is easy to know that b_1 determines the rotation direction of the orbit and $a_1 + b_2 z$ determines the convergence or divergence of the orbit.

Firstly, we take the parameters

$$a_1 = -1, \quad b_1 = 80, \quad c_1 = 18, \quad a_2 = -80,$$
$$b_2 = 1, \quad c_2 = -18, \quad a_3 = -1, \quad c_3 = 60,$$

and the initial value

$$(x_0, y_0, z_0) = (2,\ 2,\ 2).$$

When $b_1 = 80 > 0$, the rotation direction of the system orbit marked by the arrows is clockwise. When $a_1 + b_2 z > 0$ or $z > 1$, the system orbit is divergent. When $a_1 + b_2 z < 0$ or $z < 1$, the system orbit is convergent (see Fig. 5).

Subsequently, we change merely the above two parameters

$$b_1 = -80, \quad a_2 = 80,$$

and take the same initial value.

Because of $b_1 = -80 < 0$, the rotation direction of the system orbit marked by the arrows is counterclockwise. When $a_1 + b_2 z > 0$ or $z > 1$, the system orbit is divergent. When $a_1 + b_2 z < 0$ or $z < 1$, the system orbit is convergent (see Fig. 6).

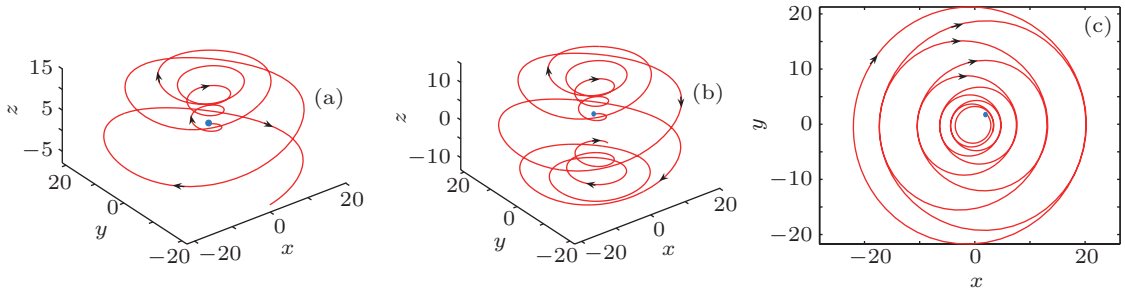


Fig. 5. (color online) The orbit of system (1): (a) $t = 0.5$ s, (b) $t = 0.8$ s, (c) projection of the orbit in the x–y plane.

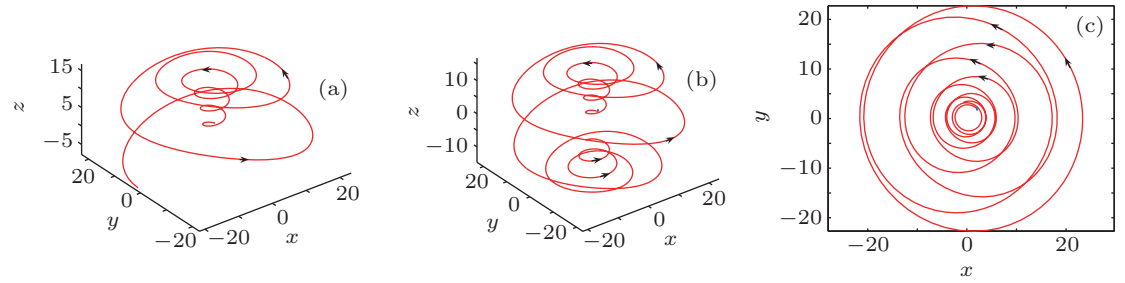


Fig. 6. (color online) The orbit of system (1): (a) $t = 0.5$ s, (b) $t = 0.8$ s, (c) projection of the orbit in the x–y plane.

3.4. Variation of parameters

Fix arbitrarily seven parameters of eight parameters ($a_1 = -1$, $b_1 = 80$, $c_1 = 18$, $a_2 = -80$, $b_2 = 1$, $c_2 = -18$, $a_3 = -1$, $c_3 = 60$), and let the residual parameter vary respectively.

1) When $-10 \le a_1 \le -0.1$, the shapes of chaotic attractors with the variation of parameter a_1 are shown in Fig. 7.

2) When $20 \le b_1 \le 200$, the shapes of chaotic attractors with the variation of parameter b_1 are shown in Fig. 8.

3) When $-400 \le c_1 \le 300$, the shapes of chaotic attractors with the variation of parameter c_1 are shown in Fig. 9.

4) When $-200 \le a_2 \le -20$, the shapes of chaotic attractors with the variation of parameter a_2 are shown in Fig. 10.

5) When $0.06 \le b_2 \le 8$, the shapes of chaotic attractors with the variation of parameter b_2 are shown in Fig. 11.

6) When $-500 \le c_2 \le 800$, the shapes of chaotic attractors with the variation of parameter c_2 are shown in Fig. 12.

7) When $-10 \le a_3 \le -0.1$, the shapes of chaotic attractors with the variation of parameter a_3 are shown in Fig. 13.

8) When $0.8 \le c_3 \le 600$, the shapes of chaotic attractors with the variation of parameter c_3 are shown in Fig. 14.

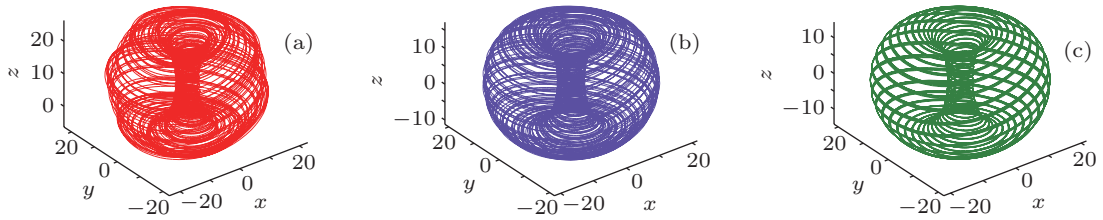


Fig. 7. (color online) Novel chaotic attractors: (a) $a_1 = -10$, (b) $a_1 = -3$, and (c) $a_1 = -0.1$.

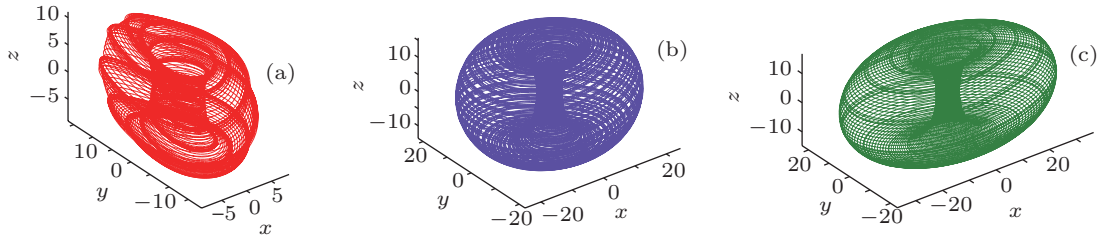


Fig. 8. (color online) Novel chaotic attractors: (a) $b_1 = 20$, (b) $b_1 = 100$, and (c) $b_1 = 200$.

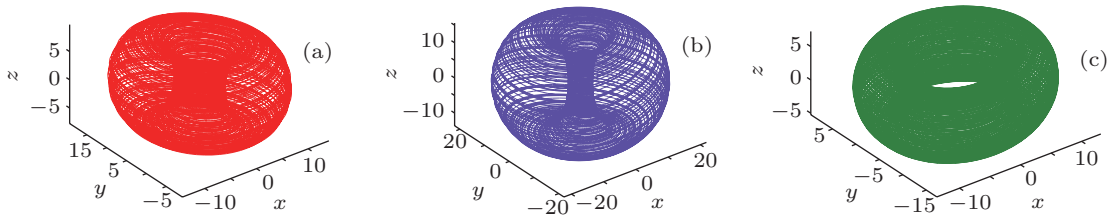


Fig. 9. (color online) Novel chaotic attractors: (a) $c_1 = -400$, (b) $c_1 = 0$, and (c) $c_1 = 300$.

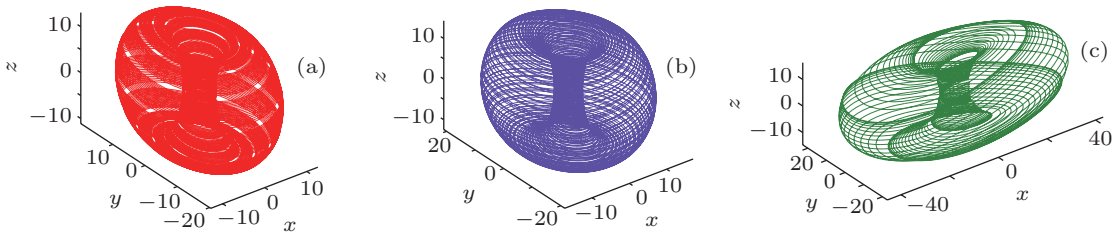


Fig. 10. (color online) Novel chaotic attractors: (a) $a_2 = -200$, (b) $a_2 = -120$, and (c) $a_2 = -20$.

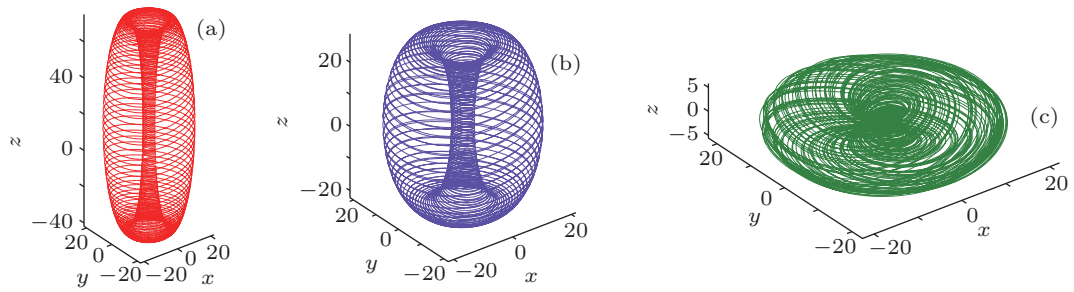


Fig. 11. (color online) Novel chaotic attractors: (a) $b_2 = 0.06$, (b) $b_2 = 0.3$, and (c) $b_2 = 8$.

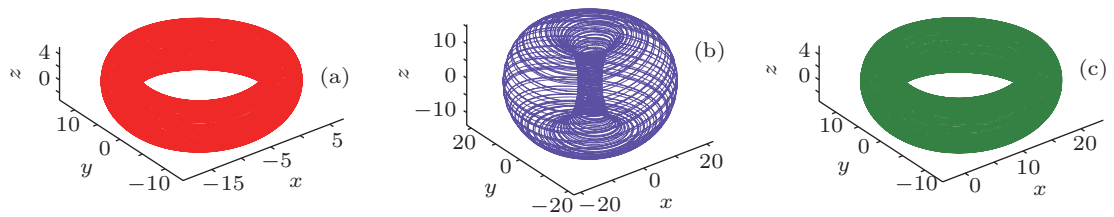


Fig. 12. (color online) Novel chaotic attractors: (a) $c_2 = -500$, (b) $c_2 = 0$, and (c) $c_2 = 800$.

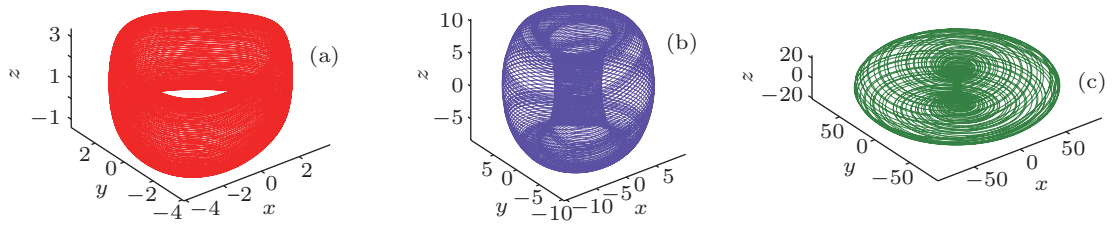


Fig. 13. (color online) Novel chaotic attractors: (a) $a_3 = -10$, (b) $a_3 = -3$, and (c) $a_3 = -0.1$.

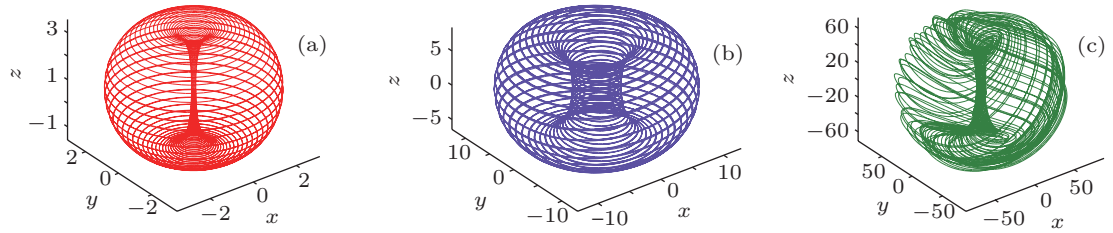


Fig. 14. (color online) Novel chaotic attractors: (a) $c_3 = 0.8$, (b) $c_3 = 28$, and (c) $c_3 = 600$.

4. The existence of spherical chaotic attractors in other 3D systems

In this section, the problem on the existence of similar spherical chaotic attractors in other 3D systems is investigated further. Compared with system (1), a simpler 3D system and a more complex 3D system with the capability of generating spherical chaotic attractors are put forward.

Firstly, the parameters of system (1) are decreased in quantity. Let

$$a_1 = c_1 = c_2 = 0,$$

a simpler 3D system is obtained as follows:

$$\begin{cases} \dot{x} = b_1 y, \\ \dot{y} = a_2 x + b_2 yz, \\ \dot{z} = a_3 y^2 + c_3. \end{cases} \tag{10}$$

(i) When $b_1 = b_2 = c_3 = 1$, $a_2 = a_3 = -1$, the system (10) becomes the first one of 19 simple chaotic systems that were found by Sprott[4] in 1994. The equation was described by[4]

$$\begin{cases} \dot{x} = y, \\ \dot{y} = -x + yz, \\ \dot{z} = 1 - y^2. \end{cases} \tag{11}$$

If the initial value is

$$(x_0, y_0, z_0) = (2,\ 2,\ 2),$$

the system (11) has a nonspherical chaotic attractor (see Figs. 15–18).

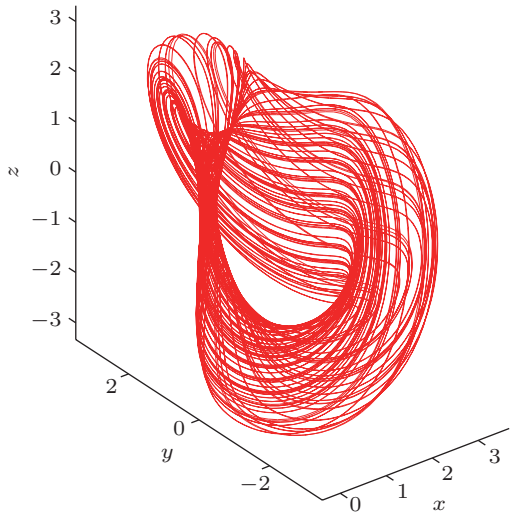


Fig. 15. (color online) A novel nonspherical chaotic attractor.

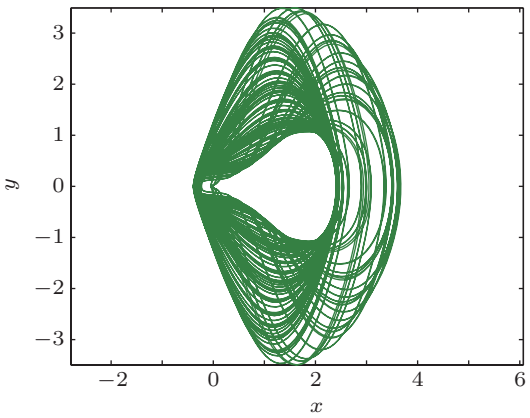


Fig. 16. (color online) Projection of the chaotic attractor in the x–y plane.

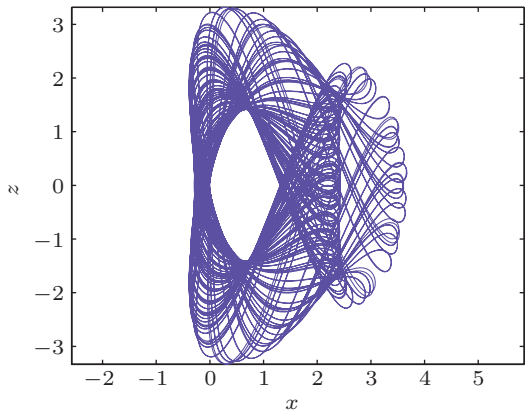


Fig. 17. (color online) Projection of the chaotic attractor in the x–z plane.

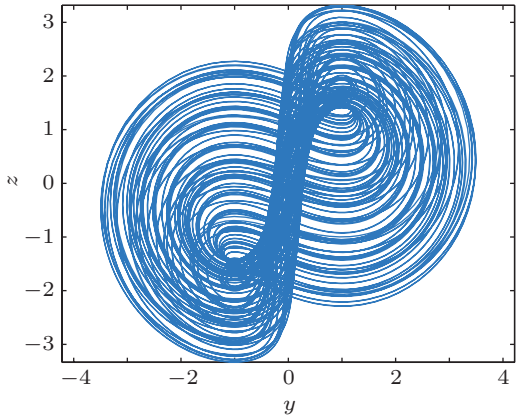


Fig. 18. (color online) Projection of the chaotic attractor in the y–z plane.

The reason that the system (11) cannot generate a spherical chaotic attractor is investigated. The Jacobian matrix $\boldsymbol{J}$ of the system (11) is

$$\boldsymbol{J} = \begin{bmatrix} 0 & 1 & 0 \\ -1 & z & y \\ 0 & -2y & 0 \end{bmatrix} = \begin{bmatrix} \boldsymbol{A} & \boldsymbol{B} \\ \boldsymbol{C} & 0 \end{bmatrix}, \tag{12}$$

where

$$\boldsymbol{A} = \begin{bmatrix} 0 & 1 \\ -1 & z \end{bmatrix}, \quad \boldsymbol{B} = \begin{bmatrix} 0 \\ y \end{bmatrix}, \quad \boldsymbol{C} = \begin{bmatrix} 0 & -2y \end{bmatrix}.$$

According to the inequality (8), we have

$$|z| < 2. \tag{13}$$

If $|z| < 2$ for $\forall z$, then $\boldsymbol{A}$ has a pair of conjugate complex eigenvalues, the system (11) may generate a spherical chaotic attractor. However, by estimating simply the boundary of z as shown in Fig. 17 or Fig. 18, $\exists z$, $|z| > 2$ holds, so $\boldsymbol{A}$ does not have a pair of conjugate complex eigenvalues when $|z| > 2$. Hence, the system (11) cannot generate a spherical chaotic attractor.

(ii) Take the parameters

$$b_1 = 100, \quad a_2 = -100, \quad b_2 = 1, \quad a_3 = -1, \quad c_3 = 80,$$

and the initial value

$$(x_0, y_0, z_0) = (2,\ 2,\ 2),$$

the system (10) can generate a novel spherical chaotic attractor(see Figs. 19–22).

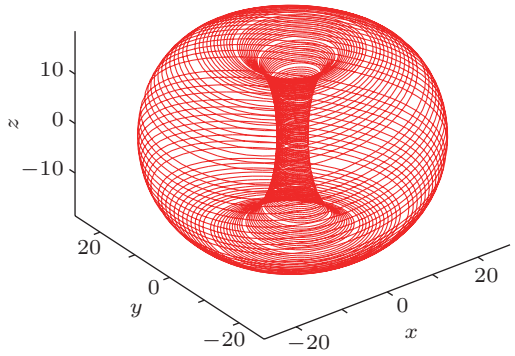


Fig. 19. (color online) A novel spherical chaotic attractor.

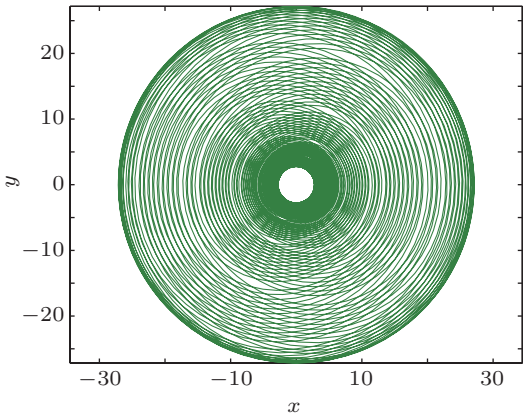


Fig. 20. (color online) Projection of the chaotic attractor in the x–y plane.

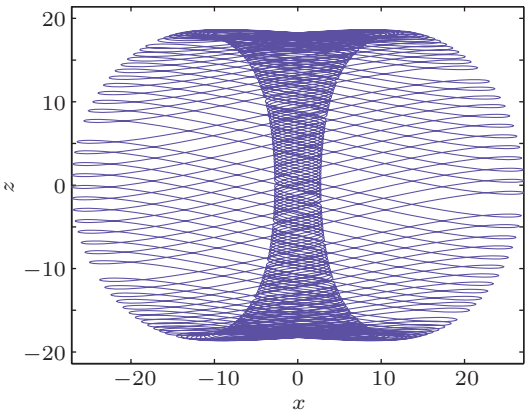


Fig. 21. (color online) Projection of the chaotic attractor in the x–z plane.

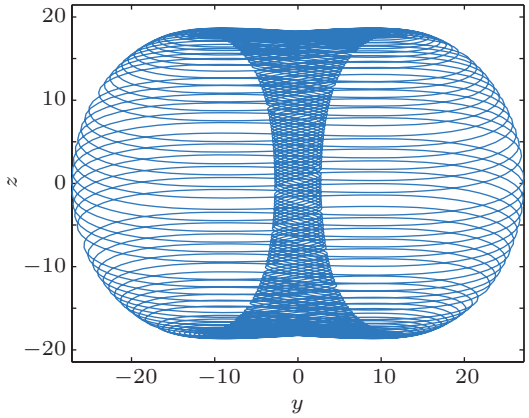


Fig. 22. (color online) Projection of the chaotic attractor in the y–z plane.

According to the inequality (8), we have

$$|z| < 200. \tag{14}$$

By estimating simply the boundary of z as shown in Fig. 21 or Fig. 22, for $\forall z$, $|z| < 200$ holds, so $\boldsymbol{A}$ has a pair of conjugate complex eigenvalues. Therefore, the system (10) with no equilibria has the capability of generating a spherical chaotic attractor under the condition of suitable parameters.

Finally, the parameters of system (1) are increased in quantity. A more complex 3D system with ten parameters and three quadratic terms is obtained as follows:

$$\begin{cases} \dot{x} = a_1 x + b_1 y + c_1, \\ \dot{y} = a_2 x + d_2 y + b_2 yz + c_2, \\ \dot{z} = a_3 y^2 + b_3 x^2 + c_3. \end{cases} \tag{15}$$

When $a_1 = -1$, $b_1 = 100$, $c_1 = 10$, $a_2 = -100$, $b_2 = 1$, $c_2 = -12$, $d_2 = 1$, $a_3 = -1$, $b_3 = -1$, $c_3 = 50$, and the initial value $(x_0, y_0, z_0) = (2,\ 2,\ 2)$, the system (15) can also generate a novel spherical chaotic attractor (see Figs. 23–26).

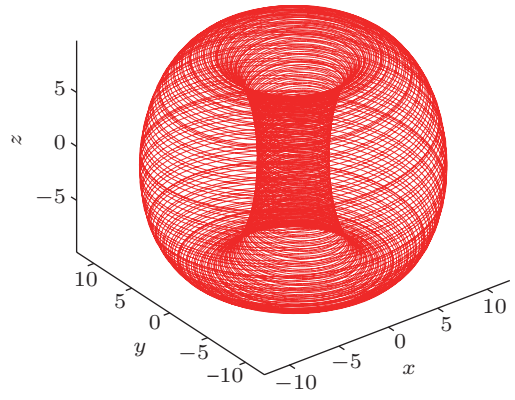


Fig. 23. (color online) A novel spherical chaotic attractor.

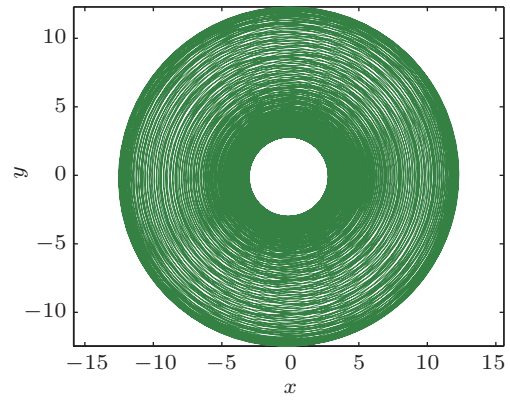


Fig. 24. (color online) Projection of the chaotic attractor in the x–y plane.

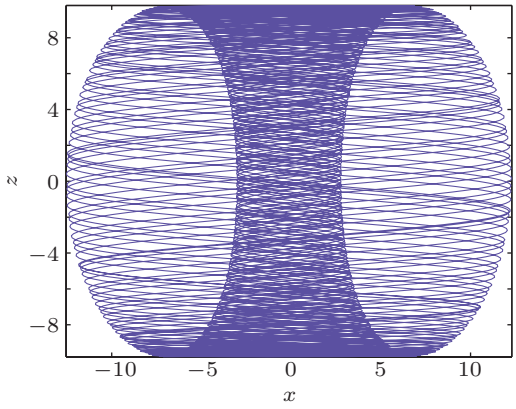


Fig. 25. (color online) Projection of the chaotic attractor in the x–z plane.

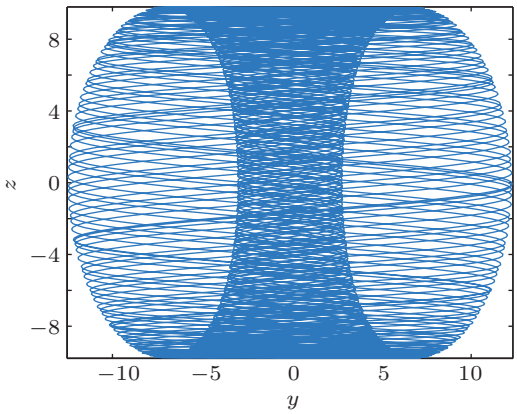


Fig. 26. (color online) Projection of the chaotic attractor in the y–z plane.

5. Conclusions

A new 3D chaotic system with eight parameters and two quadratic terms is constructed and a novel spherical chaotic attractor is generated from the system in this paper. The system has a strong capability of generating spherical chaotic attractors within a wide range of parameters. Basic dynamical behaviors of the system are investigated in detail. Finally, a simpler 3D system and a more complex 3D system with the capability of generating spherical chaotic attractors are put forward further.

References

[1] Lorenz E N 1963 *J. Atmos. Sci.* **20** 130
[2] Rössler O E 1976 *Phys. Lett. A* **57** 397
[3] Chua L O, Komuro M and Matsumoto T 1986 *IEEE Trans. Circ. Syst.* **33** 1072
[4] Sprott J C 1994 *Phys. Rev. E* **50** R647
[5] Chen G R and Ueta T 1999 *Int. J. Bifurc. Chaos* **9** 1465
[6] Lü J H and Chen G R 2002 *Int. J. Bifurc. Chaos* **12** 659
[7] Dong E Z, Chen Z P, Chen Z Q and Yuan Z Z 2009 *Chin. Phys. B* **18** 2680
[8] Cang S, Qi G and Chen Z 2010 *Nonlinear Dyn.* **59** 515
[9] Xue W, Qi G Y, Mu J J, Jia H Y and Guo Y L 2013 *Chin. Phys. B* **22** 080504
[10] Yu F, Wang C H, Yin J W and Xu H 2012 *Acta Phys. Sin.* **61** 020506 (in Chinese)
[11] Liu X Y 2009 *Chin. Phys. Lett.* **26** 090504
[12] Dadras S, Momeni H R and Qi G 2010 *Nonlinear Dyn.* **62** 391
[13] Yu F, Wang C H, Yin J W and Xu H 2011 *Chin. Phys. B* **20** 110505
[14] Yu S, Tang W K S, Lü J and Chen G 2008 *IEEE Trans. Circ. Syst. II* **55** 1168
[15] Yu S, Lü J, Chen G and Yu X 2011 *IEEE Trans. Circ. Syst. II* **58** 314
[16] Zhou X, Wang C H and Guo X R 2012 *Acta Phys. Sin.* **61** 200506 (in Chinese)
[17] He S B, Sun K H and Zhu C X 2013 *Chin. Phys. B* **22** 050506
[18] Luo M W, Luo X H and Li H Q 2013 *Acta Phys. Sin.* **62** 020512 (in Chinese)
[19] Sprott J C 2000 *Phys. Lett. A* **266** 19
[20] Li D 2008 *Phys. Lett. A* **372** 387
[21] Yang X S and Li Q 2003 *Chaos Soliton. Fract.* **18** 25
[22] Li Q, Yang X S and Yang F 2003 *Electronics Lett.* **39** 1306
[23] Lü J, Chen G, Yu X and Leung H 2004 *IEEE Trans. Circ. Syst. I* **51** 2476
[24] Lü J, Han F, Yu X and Chen G 2004 *Automatica* **40** 1677
[25] Lü J, Yu S, Leung H and Chen G 2006 *IEEE Trans. Circ. Syst. I* **53** 149
[26] Lü J, Murali K, Sinha S, Leung H and Aziz-Alaoui M A 2008 *Phys. Lett. A* **372** 3234
[27] Yu S, Lü J, Leung H and Chen G 2005 *IEEE Trans. Circ. Syst. I* **52** 1459
[28] Yu S, Lü J and Chen G 2007 *Phys. Lett. A* **364** 244
[29] Zhang C and Yu S 2010 *Phys. Lett. A* **374** 3029
[30] Lü J, Zhou T, Chen G and Yang X 2002 *Chaos* **12** 344
[31] Lü J, Yu X and Chen G 2003 *IEEE Trans. Circ. Syst. I* **50** 198
[32] Zheng Z, Lü J, Chen G, Zhou T and Zhang S 2004 *Chaos Soliton Fract.* **20** 277
[33] Yu S, Lü J and Chen G 2007 *IEEE Trans. Circ. Syst. I* **54** 2087
[34] Guo J, Xie G and Wang L 2009 *Chaos Soliton. Fract.* **40** 2160
[35] Chen Q, Hong Y, Chen G and Zhong Q 2006 *Phys. Lett. A* **348** 195
[36] Zhou T and Chen G 2004 *Int. J. Bifurc. Chaos* **14** 1795